Re-entry by Early Afterdepolarisations in a Computational Model

S Scarle, R H Clayton

Department of Computer Science, University of Sheffield, United Kingdom

Abstract

Afterdepolarisations are one mechanism suggested for the spontaneous initiation of re-entrant arrhythmias in the ventricles but are difficult to study experimentally. We have conducted a systematic investigation of the initiation of re-entry by afterdepolarisations using a computational model of cardiac ventricular tissue. We implemented a mono-domain model of a 1D fibre, where the excitability of the cell membrane was described by the 4 variable Fenton-Karma (FK4V) model. We embedded additional behaviour into the FK4V model, so a prescribed region produced afterdepolarisations. By changing the size of this region, and duration, amplitude and frequency of the afterdepolarization potentials, we were able to look in detail at how afterdepolarizations can initiate propagating action potentials. This study has shown that afterdepolarisations are capable of producing re-entry, but the duration and amplitude of the afterdepolarisation potential are important in determining whether re-entry is produced.

1. Introduction

Triggered activity is involved in many cardiac arrhythmias. The basis of such activity is an afterdepolarization or oscillation of membrane potential that occurs near the time that the cell is repolarizing. Those oscillations occurring during repolarization are known as early afterdepolarizations (EADs) and those occurring just after repolarization are known as delayed afterdepolarizations. If the membrane voltage oscillation is of sufficient magnitude that it brings the membrane potential of surrounding tissue to threshold, an extrasystole can result. A sustained reentrant arrhythmia triggered by an extrasystole is a rare event - perhaps only once in a lifetime, usually its end. It is likely that reentry occurs more often, producing self-terminating arrhythmic episodes, and recent experimental studies have shown that EADs can initiate propagating extrasystoles[1].

We have used a computational model to study how the volume of tissue generating an EAD and the coupling between the EAD capable region and the surrounding tissue effect action potential (AP) propagation in a FK4V in quasi 0-D (one or two connected cells) and 1-D simulated tissue.

2. Cell model

Cardiac tissue can be modelled as an electrically excitable medium which supports travelling waves of electrical activation or action potentials (APs). Propagating APs can be described by a non-linear reaction diffusion equation [2] leading to the monodomain tissue model

$$C_m \frac{\partial V_m}{\partial t} = \nabla . D \nabla V_m - I_{ion} \tag{1}$$

The left side of equation 1 describes current flowing due to the capacitance of the cell membrane, whilst the right gives current flow due to gradients in trans-membrane potential (diffusive term $= \nabla . D \nabla V_m$) and current flow through ion channels, pumps and transporters in the cell membrane (reaction term $= I_{ion}$). Where, $D = 0.0005$ cm^{2}ms^{-1} is the diffusion coefficient, V_m is voltage across the cell membrane, $C_m = 1\mu$Fcm^{-2} is membrane capacitance per unit area and I_{ion} is membrane current flow per unit area. We have used FK4V for I_{ion}[3].

$$I_{ion} = \frac{J_{fi} + J_{so} + J_{si}}{C_m} \tag{2}$$

Each J_x is a simulated flow of various ions across a cardiac cell membrane.The naming convention, shown in Table 1, is used to reiterate that the currents do not actually represent measured currents, but only their activation, inactivation and reactivation dynamics. It is only these dynamics that are required to qualitatively reproduce cardiac cell restitution properties. These J_x are governed by three internal variables and V_m rescaled to be a dimensionless activation,

$$U = \frac{V_m - V_0}{V_{fi} - V_0} \tag{3}$$

where $V_0 = -85$mV (resting potential) and $V_{fi} = 15$mV (Nernst potential of the fast interval current).

All simulations for this study were carried out by solving Equation 1 using a basic finite difference Euler numeric integration with a two speed time-step. The spatial and temporal steps used were $\delta x = 0.02$ cm and $\delta t = 0.1$ ms or 0.01 ms. The choice of δt for the internal degrees of freedom being based on the rate of voltage diffusion at the site under consideration.

J	description	ion
fi	fast inward	Na^+
so	slow outward	K^+
si	slow inward	Ca^+

Table 1. Description of ionic currents used in the Fenton Karma 4 variable model.

2.1. Oscillatory behaviour

It has been well established[4] that intra-cellular Ca^{2+} accumulation predisposes the myocardium to abnormal electrical activity such as EAD, but such Ca^{2+} effects a number of different membrane currents: the Na^+-Ca^{2+} exchanger current (I_{NaCa}) the L-type channel current ($I_{Ca(L)}$) and the Ca^{2+}-activated non selective current ($I_{ns(Ca)}$). Ca^{2+} handling is complex because Ca^{2+} release is very nonlinear and spatially non-uniform. Due to these multiple effects a large number of cell models including Ca^{2+} have been constructed, these often bolt on more complex calcium dynamics to previous models[5]. Another approach for modelling EAD is to alter the conductance of an ion channel to break a stable feedback and so produce oscillatory behaviour[6]. However, one problem can be distinguishing actual instabilities in behaviour and purely mathematically artifacts[7], as a minuscule change in the alteration ($\sim 0.04\%$) can cause a great change in behaviour[8].

We were interested not in how the oscillatory behaviour that leads to EADs was produced but merely on the effect of these oscillations in U on the surrounding tissue. Our normal cells were therefore governed purely by FK4V, using internal parameters which match epicardial cell behaviour. Additionally, our EAD capable simulated cells had three states as follows :-

State One: Behaved as FK4V until all these conditions were met:

$$0.5 < d < 0.6 \quad \frac{dd}{dt} < 0 \quad \dot{U}^{int} < 0 \tag{4}$$

upon which they enter State Two. Here, $\dot{U}^{int}$ indicates the rate of change in U due to the internal currents, I_{ion}. In this way the oscillatory behaviour was started before repolarization had been completed, as required for EADs.

State Two: Purely oscillatory U behaviour for a fixed duration of D ms. $\dot{U}^{int}$ being replaced with the time dependant rate of change of a simple harmonic oscillator:

$$\dot{U}^{int}(t) = -\frac{2A\pi}{P}\cos\left(\frac{2\pi(t-T)}{P}\right) \tag{5}$$

where $A =$ amplitude of oscillation, $P =$ period of oscillation and $T =$ time at which oscillation began. After time D ms cell entered State Three.

State Three: Cell returned to FK4V behaviour for the rest of the simulation.

U against time plots of a normal AP and an example EAD AP are shown in Figure 1.

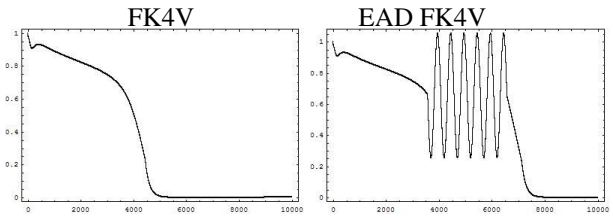

Figure 1. Comparison of normal FK4V AP and an example EAD AP. U on the y-axes and time in time-steps on the x-axes.

To reiterate, in our study we do not consider the mechanism of EADs but just their effect on the surrounding tissue. So for the majority of the time the system behaves as normal cardiac tissue, but then at some time and for a set period an oscillatory behaviour takes control of U (and U only), which we take to be a black box process. Most suggested mechanisms for EAD are based on pause dependant effects[9], so once re-entry has been initiated excitation will come around more frequently, therefore we can (to a first approximation) ignore subsequent alteration of the cells behaviour due to the oscillatory mechanism. State Three also keeps such cells from entering infinite loops where upon exiting State Two the conditions are again met and oscillation begins again. This would lead to a false positive for the production of re-entry.

3. Simulations

The multi-dimensional nature of data produced by a 3-D simulation of cardiac tissue can make it difficult to extract useful information. We therefore increased the complexity of the simulation from quasi 0-D and1-D to later simulations in higher dimensional systems, so that by analogy to the lower dimensional cases we can extract more information from the higher dimensional ones, where a full observation of the system can be difficult or even impossible. Preliminary simulations of a pair of connected simulation cells of which only one was EAD capable were carried out. Here, the full AP with oscillatory part for an EAD capable cell (see Figure 1) was seen but once it was connected to a normal cell, the voltage of the EAD cell during the oscillation was pulled down by the neighbouring normal cell if the EAD's A was too low. However, this decay could be overcome if we increased A to 0.6 or higher, but in this tightly connected system the normal cell's behaviour was totally swamped by its EAD capable neighbour. This suggests that the effects of EAD cells will have a large footprint in higher dimensional systems.

3.1. Range effect

We undertook simulations of an 0.8 cm long 1-D system. This comprised of one EAD capable grid point at the end of a line of 39 normal ones. We carried out multiple simulations which varied all aspects of the oscillatory behaviour of our EAD capable cell: D from 20 ms to 400 ms in steps of 20 ms, A from 0.2 to 1.0 in steps of 0.2 and P from 10 ms to D in steps of 10 ms. A single excitation (U set to 1) was applied at time $= 0$, to the EAD site. We produced voltage space-time plots (VSTs) from these simulations. VSTs show how U varied with both distance along the line away from the EAD cell and with time. We show the VSTs for the simulations with the following EAD parameters; $A = 1.0$, $D = 320$ ms, $P = 10 - 60$ ms (see Figure 2).

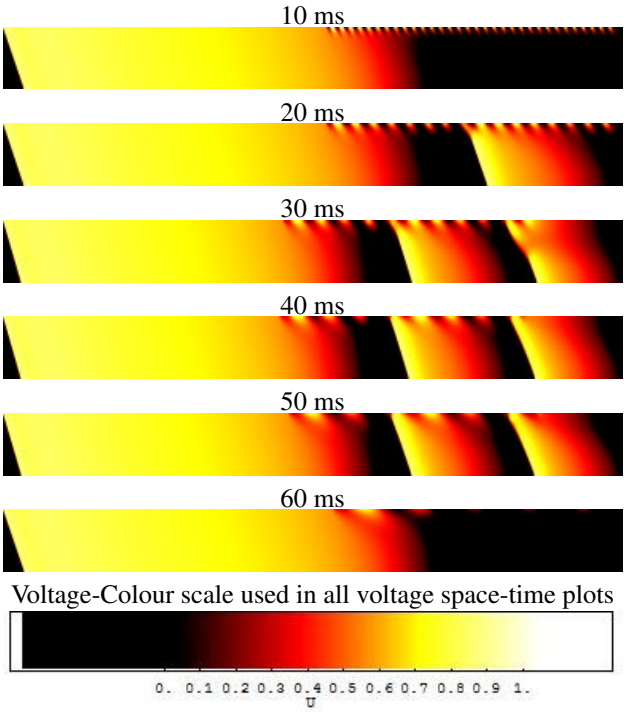

Figure 2. Voltage Space-Time plots for simulations with a single EAD capable cell at the end of a 40 simulation cell line. Times indicate the period of the oscillatory behaviour. Space is along the y-axes and time along the x-axes. The top edge of each plot is the EAD capable cell and all time axes are scaled to fill column width.

We produced behaviour diagrams for each amplitude. No set of oscillatory parameters with an $A < 0.8$ produced an extrasystole, so we show only those for $A = 0.8$ (Figure 3a) and $A = 1.0$ (Figure 3b).

The dampening effect seen in 0-D is amplified in this extended 1-D system and higher A is required for the EAD capable cell to retain a high enough U to generate an extrasystole. Similarly, it is only at lower P that we see extrasystoles as these maintain their elevated U, whilst longer P allow the voltage to leak away. Notably, even when no extrasystoles are produced the EAD capable cell still greatly effects its neighbours, driving them in step with itself. In some of the longer P simulations with no extrasystoles a range effect can still be seen into the normal tissue, in this case damping down the normal cells. This tells us that EAD capable cells can act as both sinks and sources of voltage.

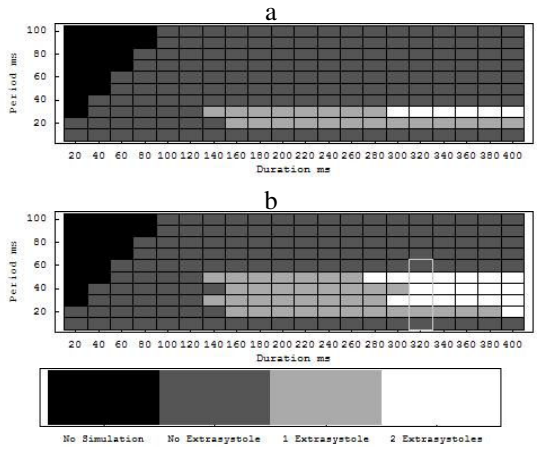

Figure 3. Behaviour diagrams for 1 EAD capable cell at the end of a 40 cell fibre; a. Amplitude = 0.8, b. Amplitude = 1.0. The highlighted region indicates parameters used for later simulations and Figure 2.

3.2. EAD-normal coupling

Computational studies have indicated that both the number of cells involved and the coupling between these cells and surrounding tissue[10] are critical in generating extrasystoles[11]. This idea is similar to the concept of liminal length in neuronal propagation. Under some conditions the oscillatory activity may persist and there may be a burst of extrasystoles leading to a burst of tachycardia. Therefore, we considered what would happen if the coupling between the EAD capable cells was reduced and how the size of the EAD capable region would affect overall behaviour. Our second set of simulations used a 5cm long 1-D system of 250 simulation cells with zero-flux end conditions. In this system a section of the line from 100 to $100 + l$ cells (l being varied in steps of 10 from $l = 10$ to $l = 100$) were EAD capable and the two ends of this EAD zone had their diffusion coefficients set to multiples of $1/10$ of the normal value. The first cell was excited as before, and the system was simulated until all U returned to their resting value and all EAD capable cells had reached state three. For the parameters of the oscillatory behaviour

in the EAD zone we used those highlighted previously. If the EAD is super-threshold and occurs in the vulnerable window, retrograde propagation will occur in a 1-D virtual tissue[12]. The addition of our oscillatory EAD behaviour could trigger either bidirectional or unidirectional propagation, and the unidirectional propagation could be either retrograde or antegrade. We observed that the afterdepolarisation region (i) produced an afterdepolarisation but no propagating activity, (ii) produced an AP propagating in a retrograde direction, (iii) produced an AP propagating in an antegrade direction, or (iv) produced an AP propagating in both antegrade and retrograde directions. Multiple propagating APs in either direction could be created within in the same simulation. In 2D and 3D tissue these behaviours would correspond to abnormal repolarization, re-entry, a premature ventricular beat or a mixture of the two.

4. Comparison to 1D

When we extend our system into 2 and 3-D, we clearly gain a greater degree of freedom by which our EAD capable cells can lead to re-entry. The EAD region can act as a source of excitation to nearby recovered tissue or the EAD region (due to its longer time to reach recovery) can act as a block. 2-D simulations were done with a layout which extended our 1-D runs, so the latter would be a cross-section of the former. The EAD zone now being a circle, and to ensure it was completely contained, the differing diffusion constant area was widened to three simulation cells. 3-D simulations had a spherical EAD zone. Pilot simulations have shown that the 1D results are broad predictors of behaviour in higher dimensional models. However, EAD zone size effects are weaker at lower dimensions, and in 1-D can be swamped by conduction delay caused by the differing diffusion coefficients. Although, even in 1-D size effects were still observed. Small EAD regions, with short, high frequency and low amplitude potentials tended to produce no propagating activity, whereas larger regions with longer, lower frequency, and higher amplitude potentials did produce propagating action potentials. However, if the frequency became too low we once again lost propagating activity as the surrounding tissue suppressed the EAD oscillations.

Acknowledgements

We would like to thank the British Heart Foundation for funding this work (PG/03/102/1582) and the Integrative Biology eScience project (EPSRC GR/S72023/01) for their computer time.

References

[1] Choi BR, Burton F, Salama G. Cytosolic Ca^{2+} triggers early afterdepolarisations and Torsade de Pointes in rabbit hearts with type 2 long QT syndrome. Journal of Physiology 2002;543:615–631.

[2] Clayton RH. Computational models of normal and abnormal action potential propagation in cardiac tissue: Linking experimental and clinical cardiology. Physiological Measurement 2001;22:R15–R34.

[3] Fenton F, Karma A. Vortex dynamics in three-dimensional continuous myocardium with fibre rotation: Filament instability and fibrillation. Chaos 1998;8:20–47.

[4] Wit AL, Janse M. The ventricular arrhythmias of ischemia and infraction. New York: Futura, 1993.

[5] Chudin E, Goldhaber J, Garfinkel A, Weiss J, Kogar B. Intracellular Ca^{2+} Dynamics & the Stability of Ventricular Tachycardia. Biophysical J 1999;77:2930–2941.

[6] Nordin C. Computer Model of electrophysiological instabilities in very small heterogeneous ventricular syncytia. Am J Physiol Heart and Circ Physiol 1997;272:H1838–H1856.

[7] Luo CH, Rudy Y. A dynamic model of the cardiac ventricular action potential I. Simulations of ionic currents and concentration changes. Circ Res 1994;74:1071–96.

[8] Clayton RH, Holden AV, Tong WC. Can endogenous, noise-triggered early after-depolarisations initiate reentry in a modified Luo-Rudy virtual tissue? Int J of Bifurcation and Chaos 2003;13:3885–3843.

[9] Zhou JT, Zhang LR, Liu WY, Zhang GL, Jing Z, Shi JL, Wang ZY, Zhang YS. Early Afterdepolarizations in the familial QTU Syndrome. J of Cardiovascular Electrophysiology 1992;3:431–436.

[10] A.P.Henriquez, Vogel R, Muller-Borer B, Henriquez C, Weingart R, Cascio W. Influence of dynamic gap junction resistance on impulse propagation in ventricular myocardium: A computer simulation study. Biophysical Journal 2001;81:2112–2121.

[11] Winslow R, Varghese A, Noble D, Adlakha C, Hoythya A. Generation and propagation of ectopic beats induced by spatially localised Na-K pump inhibition in atrial networks. Proceedings of the Royal Society of London B 1993; 254:55–61.

[12] Shaw RM, Rudy Y. The vulnerable window for unidirectional block in cardiac tissue: Characterization and dependence on membrane excitability and intercellular coupling. J Cardiovasc 1995;6:115–131.

Address for correspondence:

Dr R. H. Clayton, e-mail: r.h.clayton@sheffield.ac.uk.
Department of Computer Science, University of Sheffield,
Regent Court, 211 Portobello Street, Sheffield,
S1 4DP, UK.